

## Helicates

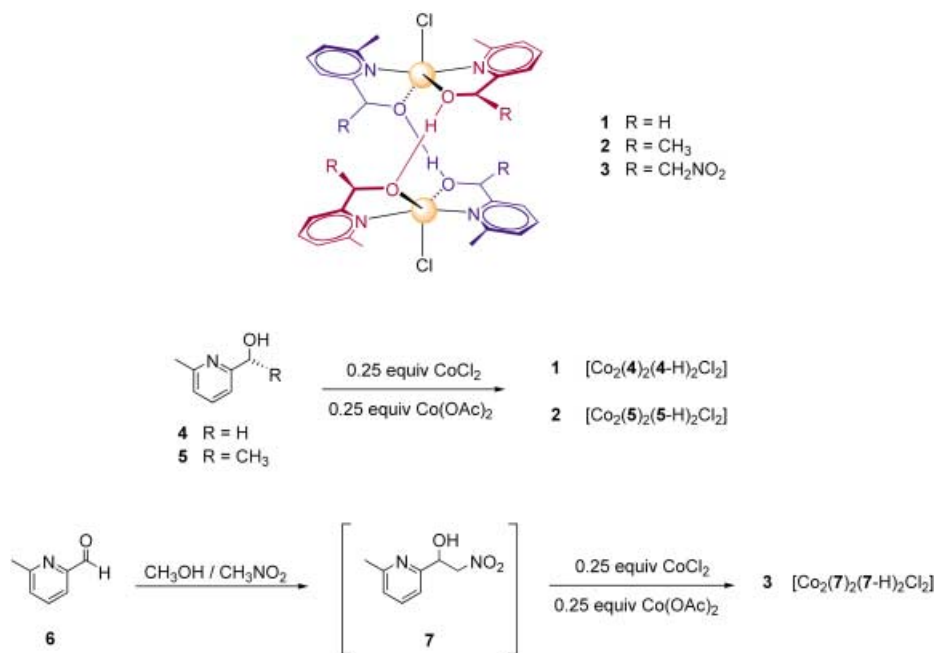
# Noncovalent Ligand Strands for Transition-Metal Helicates: The Straightforward and Stereoselective Self-Assembly of Dinuclear Double-Stranded Helicates Using Hydrogen Bonding\*\*

Shane G. Telfer,\* Tomohiro Sato, and Reiko Kuroda\*

Transition-metal helicates have played a central role in supramolecular chemistry for many years.<sup>[1–3]</sup> The synthetic approach to these structures typically follows a two-step process: 1) The synthesis of a covalent organic ligand using classical methods prior to 2) the reaction of this ligand with suitable metal ions to assemble the desired helicate. The first step in this process is often rather laborious and inefficient, especially compared to the second step which, in general, takes advantage of the kinetic lability of metal–ligand bonds to ensure that the most thermodynamically stable product is formed rapidly and in high yield. Given the obvious advantages of this noncovalent self-assembly step, it is somewhat surprising that noncovalent approaches to step 1, the construction of the ligand strands, have been reported only rarely. In these few cases metal ions were used as structural units in the ligand strands of triple helicates<sup>[4]</sup> and mesocates.<sup>[5,6]</sup> In the present paper we would like to report on a novel, noncovalent strategy for the construction of ligand strands for a series of dinuclear double helicates. This strategy utilizes hydrogen bonding between simple pyridine-alcohol precursors to build up the ligand backbone, and we show that the self-assembly of these helicates proceeds with high stereoselectivity.

Helicate **1** self-assembles upon mixing commercially available 6-methylpyridine-2-methanol (**4**) with 0.25 equivalents each of cobalt(II) chloride and cobalt(II) acetate in methanol (Scheme 1). Crimson-colored crystals of the com-

plex were obtained in high yield by layering this solution with dioxane. Helicate **2** was prepared from *R*-6-methylpyridine-2-ethanol (**5**) in an analogous fashion. This chiral starting material was obtained in 93% *ee* by the asymmetric reduction of 2-acetyl-6-methylpyridine using the general method of Ikariya and co-workers.<sup>[7]</sup> 6-Methylpyridine-2-nitromethanol (**7**), which serves as the precursor to helicate **3**, was generated in situ by the Henry reaction<sup>[8,9]</sup> of 6-methylpyridine-2-carboxaldehyde (**6**) with nitromethane. This reaction is probably catalysed by the acetate ions that are present as



**Scheme 1.** The straightforward synthetic route to helicates **1–3**. Compound **7**, which serves as a precursor to helicate **3**, is prepared in situ. The cobalt(II) centers of the helicates are colored orange and the ligand strands are shown in different colors for emphasis.

Co(OAc)<sub>2</sub>. Details of all experimental procedures are given in the Supporting Information.

The three helicates **1–3** were characterized in the solid state by X-ray crystallography (discussed below), elemental analysis, UV/Vis and IR spectroscopy, and, in the case of **2**, solid-state circular dichroism (CD) spectroscopy (see Supporting Information for details). The yield of helicate **1** is high (71%), however the yields of **2** (27%) and **3** (18%) are more modest. Monitoring of the self-assembly process of **2** in solution indicates quantitative formation of the helicate,<sup>[10]</sup> thus it appears that the crystallization step is responsible for the low yield, and we are currently exploring a variety of methods to improve upon this. It is noteworthy that the presence of a methyl substituent at the 6-position of the pyridine ring appears to be essential for the assembly of the helicates (all experiments performed using unsubstituted pyridyl starting materials led to the formation of other products).

The crystal structure of **1** (Figure 1) reveals that a pair of pyridine-methanol molecules **4** are hydrogen-bonded via their oxygen atoms to form a bisbidentate ligand strand.

[\*] Dr. S. G. Telfer, T. Sato, Prof. Dr. R. Kuroda  
JST ERATO Kuroda Chiromorphology Project  
Park Building, 4-7-6 Komaba, Meguro-ku  
Tokyo 153-0041 (Japan)  
Fax: (+81) 3-5465-0104  
E-mail: shane.telfer@chiromor2.erate.rcast.u-tokyo.ac.jp  
ckuroda@mail.ecc.u-tokyo.ac.jp

[\*\*] We thank Dr. T. Harada for help with the spectropolarimetry measurements and Dr Y. Imai for performing the HPLC analyses. The Japan Society for the Promotion of Science (JSPS) provided a post-doctoral fellowship to S.G.T.

Supporting information for this article is available on the WWW under <http://www.angewandte.org> or from the author.

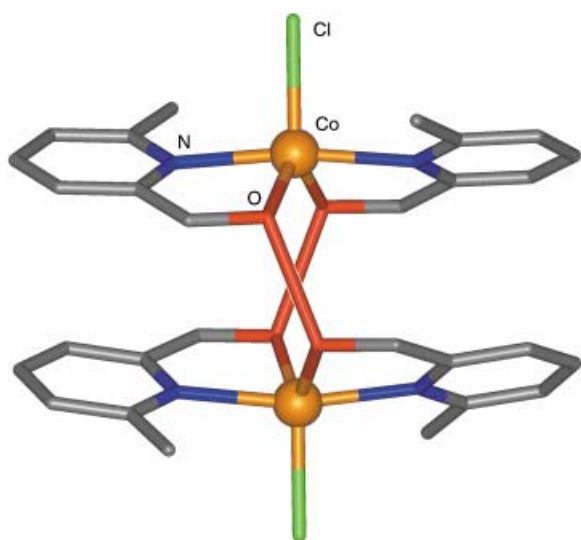


**Figure 1.** The X-ray crystal structure of the *P* enantiomer of helicate **1**. The hydrogen bonds between the oxygen atoms, which are used to build up the ligand strands, are shown in red. The other hydrogen atoms have been omitted for clarity.

Two such strands wrap around an axis defined by two cobalt(II) ions to give a dinuclear double-stranded helicate. A chloride ion completes the coordination sphere of each metal center. One proton has been lost from each ligand strand so the hydrogen bonds are of the alkoxide–alcohol type<sup>[11]</sup> and overall the helicate is neutrally charged. The separation of the two oxygen atoms is 2.42 Å, which indicates a very strong bonding interaction.<sup>[12]</sup> The use of hydrogen bonding as a construction element for the ligand strands represents the unique feature of these helicates. This truly supramolecular approach is simple, rapid, and high yielding. It also renders the covalent synthesis of a ligand strand unnecessary, and provides access to ligands that may be impossible to synthesize via conventional means.

The solid-state structures of **2** and **3** have also been determined by X-ray crystallography (Table 1). All three helicates have similar overall structures. In all cases, the pentacoordinate cobalt(II) centers adopt a distorted trigonal-

bipyramidal geometry and the internuclear separations fall in the range 4.33–4.43 Å. All three helicates possess approximate  $D_2$  symmetry, however only one twofold axis is crystallographically imposed in each structure. The alignment of this crystallographic axis determines whether the “upper and lower” (**2**) or “left and right” (**1** and **3**) halves of the helicates are symmetry related. Two pyridine rings belonging to different ligand strands and coordinated to different metal centers are found to be nearly parallel, with a separation of around 3.55 Å. This indicates a stabilizing  $\pi$ – $\pi$  interaction and is highlighted by the space-filling model of **1** (Figure 2). Figure 3 presents a diagram of **2** and a view down the Co···Co axis (the structure of **3** is included as Supporting Information).

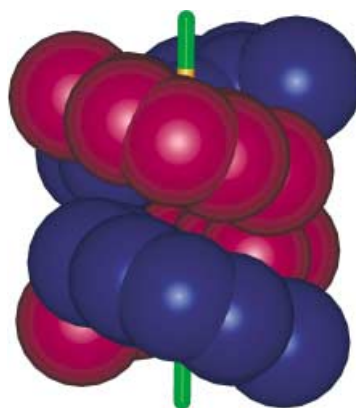


**Figure 2.** Space-filling diagram of the *P* enantiomer of helicate **1**. The ligand strands are colored differently for emphasis.

Helicates are intrinsically chiral and can be assigned the stereochemical descriptors *P* or *M* depending on whether the ligand strands describe a right- or left-handed helix. This helicity can be directly correlated with the absolute configurations of the metal centers, and in the case of helicates **1–3** the  $\Delta,\Delta$  configuration gives rise to a *P* helix. As the ligand strands of helicate **1** are achiral, this complex exists as a simple mixture of *P* ( $\Delta,\Delta$ ) and *M* ( $\Delta,\Delta$ ) enantiomers. On the other hand, the ligand strands of helicates **2** and **3** each feature two asymmetric carbon centers. These can have either *R* or *S* stereochemistry, therefore there are seven potential ligand sets for these helicates: ligand strand A/ligand strand B = *RR/RR*, *SS/SS*, *RR/RS*, *RS/SS*, *RR/SS*, *RS/RS*, and *RS/SR*. As each ligand set could lead to either a *P* helicate or an *M* helicate, there are seven pairs of enantiomers for each helicate. It is also possible that a mesocate structure may form, in which the two metal centers have opposite absolute configurations. There are a further ten distinct mesocate stereoisomers (four pairs of enantiomers and two achiral stereoisomers) which means that there is a total of 24 stereoisomers of helicates **2** and **3**.

In the synthesis of helicate **3**, the precursor compound **7** is formed in situ and will be present as a racemic mixture of *R* and *S* isomers. The X-ray crystal structure shows that the self-assembly reaction is remarkably stereoselective as only one

**Table 1:** Selected crystallographic data for helicates **1–3**.

	<b>1</b>	<b>2</b>	<b>3</b>
Selected separations [Å]			
Co–Co	4.38	4.33	4.43
O–O	2.42	2.42–2.44	2.42
Co–N	2.14–2.15	2.13–2.15	2.14–2.17
Co–O	1.99–2.00	1.96–2.00	2.00
Co–Cl	2.31–2.34	2.34	2.30–2.31
Selected angles [°]			
N–Co–N	168.8 (av)	170.1	170.3 (av)
O–Co–O	115.8 (av)	120.9	115.4 (av)
O–H–O	173.3	179.9	177.0
crystallographic $C_2$ axis	Co–Co axis	$\perp$ to Co–Co axis	Co–Co axis

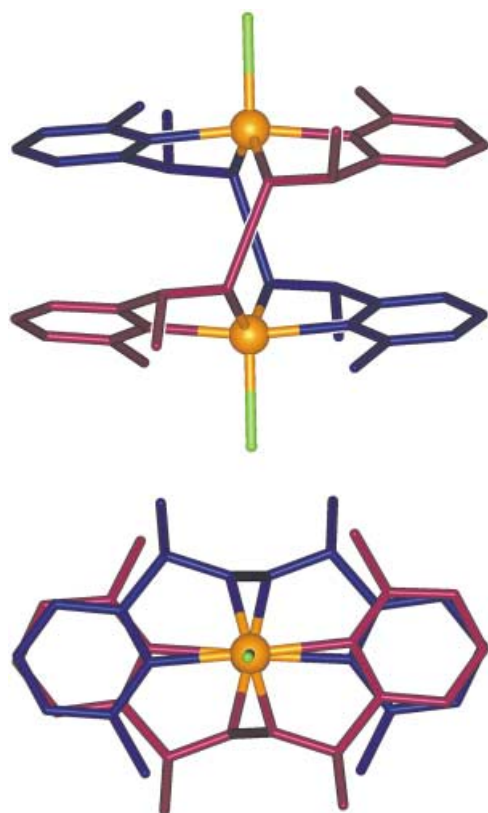


**Figure 3.** Two views of the X-ray crystal structure of helicate **2**. Above: The overall structure highlighting the orientations of the methyl groups of the ligand strands; below: a view along the Co...Co axis. The hydrogen atoms have been omitted for clarity.

pair of enantiomers, namely,  $\Delta,\Delta$ -(*SS/SS*) and  $\Lambda,\Lambda$ -(*RR/RR*), is actually observed. This demonstrates that 1) homochiral ligand sets are favored over heterochiral ligand sets, and 2) that the absolute configurations of the cobalt(II) centers are “predetermined” by the chirality of the ligands.<sup>[13]</sup> With respect to observation 1), similar self-sorting processes based on chirality have been reported for other helicates<sup>[14]</sup> and for mononuclear complexes.<sup>[15]</sup> Observation 2) is readily explained on steric grounds; a model of **3** shows that the  $\Lambda,\Lambda$ -*SS/SS* diastereomer (which does not form) would have the nitromethyl arms of one ligand strand pointing directly towards one of the pyridine rings of the other ligand strand.

In the case of helicate **2**, the sample of compound *R*-**5** that was used for its synthesis had an *ee* of 93%. Therefore, statistically the *RR/RR* ligand set will be highly favored and indeed the enantiopure *RR/RR*-**2** helicate was observed in the X-ray crystal structure. As expected on the basis of the results discussed above for helicate **3**, this ligand set induces the  $\Lambda$  configuration at both metal centers. A sample of compound *R*-**5** that was extracted from crystals of **2** had an *ee* of 100%, as indicated by chiral HPLC analysis. Thus the assembly of **2** functions as method of providing an enantiopure form of this compound, albeit a rather inefficient one due to the modest yield of the helicate. The solid-state CD spectrum<sup>[16,17]</sup> of helicate **2** is presented in Figure 4.

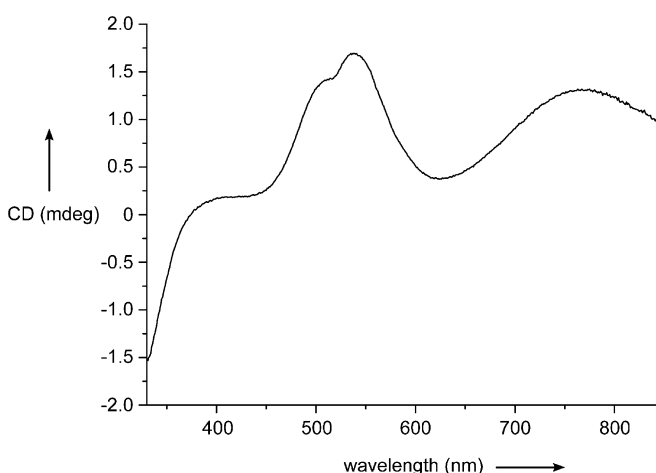


**Figure 4.** The CD spectrum of **2** in the visible region, measured in the solid state as a KBr disc.

These observations raise some interesting questions regarding the mechanisms of the self-assembly of these helicates and of the homochiral ligand-sorting process. Given the noncovalent nature of the ligand strand, it is likely that their mechanism of self-assembly differs considerably from conventional helicates. One intuitive hypothesis is that a stepwise assembly route is followed, in which precursor mononuclear complexes, for example, [CoL(L-H)Cl] (L = **4**, **5**, or **7**), are formed initially. Dimerization of such complexes would produce the observed helicates. We speculate that the observed self-sorting of the homochiral ligand may result from the stereospecific dimerization of homochiral monomers. The precise nature of the assembly process is likely to be of interest in the context of hierarchical self-assembly and we hope to report more details in the near future.

In summary, we have presented a novel and straightforward approach to transition-metal helicates by employing hydrogen bonding as a construction element for the ligand strands. The helicates self-assemble from eight simple components (four ions and four small molecules) and are stabilized by a range of supramolecular interactions: coordination bonds, hydrogen bonds, and  $\pi$ - $\pi$  interactions. This genuinely supramolecular approach to the synthesis of transition-metal helicates has obvious advantages over traditional methods, which often require the tedious synthesis of covalent ligands. Furthermore, the self-assembly process exhibits remarkable stereoselectivity: only homochiral ligand sets are observed and the chirality of these ligands efficiently predetermines the absolute configuration of the metal centers. The present paper complements other recent advances in the fields of catalysis,<sup>[18]</sup> coordination polymers,<sup>[19,20]</sup> and other supramolecular assemblies,<sup>[21–24]</sup> which benefit from a fruitful combination of coordination and hydrogen bonding. Due to the labile nature of the chloro ligands these helicates have great promise as building blocks for metal-organic coordination networks; an avenue of research we are actively pursuing.

## Experimental Section

Crystal data: CCDC 219398–219400 contain the supplementary crystallographic data for this paper. These data can be obtained free of charge via [www.ccdc.cam.ac.uk/conts/retrieving.html](http://www.ccdc.cam.ac.uk/conts/retrieving.html) (or from the Cambridge Crystallographic Data Centre, 12, Union Road, Cambridge CB21EZ, UK; fax: (+44)1223-336-033; or deposit@ccdc.cam.ac.uk).

**1·2H<sub>2</sub>O** (C<sub>28</sub>H<sub>34</sub>Cl<sub>2</sub>Co<sub>2</sub>N<sub>4</sub>O<sub>4</sub>·2H<sub>2</sub>O, *M<sub>r</sub>* = 715.38), 0.50 × 0.25 × 0.10 mm, orthorhombic, *Pbcn*, *a* = 14.4508(7), *b* = 15.1817(8), *c* = 13.5843(7) Å, *α* = *β* = *γ* = 90°, *V* = 2980.2(3) Å<sup>3</sup>, *Z* = 4, *ρ*<sub>calcd</sub> = 1.594 mg m<sup>−3</sup>, *F*(000) = 1480, radiation λ(MoK<sub>α</sub>) = 0.71073 Å, *T* = 135 K, reflections collected/unique: 17654/3495, *R*<sub>int</sub> = 0.025. Data acquired with Lorentzian, polarization, and absorption corrections (*μ* = 1.342 mm<sup>−1</sup>, *T*<sub>min</sub> = 0.55, *T*<sub>max</sub> = 0.88). Structure solved by direct methods (SHELXS-97) and refined by a full-matrix least-squares method on |*F*|<sup>2</sup> using anisotropic displacement parameters for all non-hydrogen atoms (SHELXL-97). The hydrogen atom involved in hydrogen bonding (H19) was found on the electron-density difference map. All other hydrogen atoms were placed in calculated positions. Final *R* factor for 3495 reflections (*I* > 2σ(*I*)) with 193 parameters was 0.050 (*R*<sub>w</sub> = 0.15). GOF = 1.20, max./min. residual electron density = 1.94/−0.93 Å<sup>−3</sup>.

**2·2CH<sub>3</sub>OH** (C<sub>32</sub>H<sub>42</sub>Cl<sub>2</sub>Co<sub>2</sub>N<sub>4</sub>O<sub>4</sub>·2CH<sub>3</sub>OH, *M<sub>r</sub>* = 799.54), 0.25 × 0.20 × 0.20 mm, orthorhombic, *P2<sub>1</sub>2<sub>1</sub>2*, *a* = 11.4404(15), *b* = 17.704(2), *c* = 9.4371(12) Å, *α* = *β* = *γ* = 90°, *V* = 1911.4(4) Å<sup>3</sup>, *Z* = 2, *ρ*<sub>calcd</sub> = 1.39 mg m<sup>−3</sup>, *F*(000) = 836, radiation λ(MoK<sub>α</sub>) = 0.71073 Å, *T* = 100 K, reflections collected/unique: 11411/4315, *R*<sub>int</sub> = 0.031. Data acquired with Lorentzian, polarization, and absorption corrections (*μ* = 1.054 mm<sup>−1</sup>, *T*<sub>min</sub> = 0.78, *T*<sub>max</sub> = 0.82). Structure solved by direct methods (SHELXS-97) and refined by a full-matrix least-squares method on |*F*|<sup>2</sup> using anisotropic displacement parameters for all non-hydrogen atoms (SHELXL-97). The hydrogen atoms involved in hydrogen bonding (H9 and H19) were found on the electron-density difference map. All other hydrogen atoms were placed in calculated positions. Final *R* factor for 4315 reflections (*I* > 2σ(*I*)) with 224 parameters was 0.065 (*R*<sub>w</sub> = 0.14). GOF = 1.19, max./min. residual electron density = 0.81/−1.10 Å<sup>−3</sup>, Flack parameter = 0.09(3).

**3·2CH<sub>3</sub>NO<sub>2</sub>** (C<sub>34</sub>H<sub>38</sub>Cl<sub>2</sub>Co<sub>2</sub>N<sub>8</sub>O<sub>8</sub>·2CH<sub>3</sub>NO<sub>2</sub>, *M<sub>r</sub>* = 1037.55), 0.20 × 0.12 × 0.06 mm, monoclinic, *C2/c*, *a* = 19.6707(13), *b* = 14.4567(10), *c* = 16.7018(11) Å, *β* = 110.7210(10)°, *V* = 4442.3(5) Å<sup>3</sup>, *Z* = 4, *ρ*<sub>calcd</sub> = 1.551 mg m<sup>−3</sup>, *F*(000) = 2136, radiation λ(MoK<sub>α</sub>) = 0.71073 Å, *T* = 120 K, reflections collected/unique: 13742/5130, *R*<sub>int</sub> = 0.048. Data acquired with Lorentzian, polarization, and absorption corrections (*μ* = 0.95 mm<sup>−1</sup>, *T*<sub>min</sub> = 0.83, *T*<sub>max</sub> = 0.95). Structure solved by direct methods (SHELXS-97) and refined by a full-matrix least-squares method on |*F*|<sup>2</sup> using anisotropic displacement parameters for all non-hydrogen atoms (SHELXL-97). The hydrogen atom involved in hydrogen bonding (H9) was found on the electron-density difference map. All other hydrogen atoms were placed in calculated positions. Final *R* factor for 4154 reflections (*I* > 2σ(*I*)) with 298 parameters was 0.056 (*R*<sub>w</sub> = 0.12). GOF = 1.14, max./min. residual electron density = 0.85/−1.09 Å<sup>−3</sup>.

Received: September 10, 2003 [Z52833]

**Keywords:** enantioselectivity · helical structures · noncovalent interactions · self-assembly · supramolecular chemistry

- [5] X. Sun, D. W. Johnson, D. L. Caulder, R. E. Powers, K. N. Raymond, E. H. Wong, *Angew. Chem.* **1999**, *111*, 1386; *Angew. Chem. Int. Ed.* **1999**, *38*, 1303.
- [6] X. Sun, D. W. Johnson, D. L. Caulder, K. N. Raymond, E. H. Wong, *J. Am. Chem. Soc.* **2001**, *123*, 2752.
- [7] K. Okano, K. Murata, T. Ikariya, *Tetrahedron Lett.* **2000**, *41*, 9277.
- [8] L. Henry, *C. R. Hebd. Seances Acad. Sci.* **1895**, *120*, 1265.
- [9] R. S. Varma, R. Dahiyal, S. Kumar, *Tetrahedron Lett.* **1997**, *38*, 5131.
- [10] S. G. Telfer, unpublished results.
- [11] G. A. Jeffrey, *An Introduction to Hydrogen Bonding*, Oxford University, New York, **1997**.
- [12] J. Emsley, *Chem. Soc. Rev.* **1980**, *9*, 91.
- [13] U. Knof, A. von Zelewsky, *Angew. Chem.* **1999**, *111*, 312; *Angew. Chem. Int. Ed.* **1999**, *38*, 303.
- [14] M. A. Masood, E. J. Enemark, T. D. P. Stack, *Angew. Chem.* **1998**, *110*, 973; *Angew. Chem. Int. Ed.* **1998**, *37*, 928.
- [15] S. G. Telfer, A. F. Williams, G. Bernardinelli, *Chem. Commun.* **2001**, 1498.
- [16] R. Kuroda in *Circular Dichroism*, 2nd ed. (Eds.: N. Berova, K. Nakanishi, R. W. Woody), Wiley-VCH, New York, **2000**, p. 159.
- [17] R. Kuroda, T. Harada, Y. Shindo, *Rev. Sci. Instrum.* **2001**, *72*, 3802.
- [18] B. Breit, W. Seiche, *J. Am. Chem. Soc.* **2003**, *125*, 6608.
- [19] R. Sekiya, S. Nishikiori, *Chem. Commun.* **2001**, 2612.
- [20] A. M. Beatty, *Coord. Chem. Rev.* **2003**, *246*, 131.
- [21] T. B. Norsten, K. Chichak, N. R. Branda, *Chem. Commun.* **2001**, 1794.
- [22] M. H. Al-Sayah, N. R. Branda, *Chem. Commun.* **2002**, 178.
- [23] T. D. Hamilton, G. S. Papaefstathiou, L. R. MacGillivray, *J. Am. Chem. Soc.* **2002**, *124*, 11606.
- [24] Z. Qin, M. C. Jennings, R. J. Puddephatt, *Chem. Commun.* **2001**, 2676.

[1] C. Piguet, G. Bernardinelli, G. Hopfgartner, *Chem. Rev.* **1997**, *97*, 2005.

[2] M. Albrecht, *Chem. Rev.* **2001**, *101*, 3457.

[3] A. F. Williams, *Chem. Eur. J.* **1997**, *3*, 15.

[4] M. H. W. Lam, S. T. C. Cheung, K.-M. Fung, W.-T. Wong, *Inorg. Chem.* **1997**, *36*, 4618.